Available online at www.sciencedirect.com
ScienceDirect
Bioorganic & Medicinal Chemistry Letters 18 (2008) 2362–2367
Bioorganic & Medicinal Chemistry Letters

Structure-based design and synthesis of benzimidazole derivatives as dipeptidyl peptidase IV inhibitors

Michael B. Wallace,* Jun Feng, Zhiyuan Zhang, Robert J. Skene, Lihong Shi, Christopher L. Caster, Daniel B. Kassel, Rongda Xu and Stephen L. Gwaltney, II

Takeda San Diego, Drug Discovery, 10410 Science Center Drive, San Diego, CA 92121, USA

Received 13 January 2008; revised 25 February 2008; accepted 27 February 2008
Available online 4 March 2008

Abstract—A novel series of non-covalent, benzimidazole-based inhibitors of DPP-4 has been developed from a small fragment hit using structure-based drug design. A highly versatile synthetic route was created for the development of SAR, which led to the discovery of potent and selective inhibitors with excellent pharmaceutical properties.

Dipeptidyl peptidase IV (DPP-4) is a serine protease that cleaves *N*-terminal dipeptides from polypeptides having Pro (or Ala) at the penultimate position.[1] DPP-4 rapidly cleaves and inactivates the incretin glucagon-like peptide 1 (GLP-1) in the blood. The active form of GLP-1 enhances glucose-stimulated insulin release from beta cells in the pancreas. Inhibition of DPP-4 can serve as an indirect way to increase the levels of circulating GLP-1, and it has been shown to increase insulin secretion and effectively regulate blood glucose levels.[2] DPP-4 inhibitors are highly effective therapeutic agents in the treatment of type 2 diabetes.[3] Clinical validation has been established with the FDA approval of sitagliptin (Januvia™),[4] as well as the progression of several other candidates through advanced stages of development.[5]

Numerous classes of DPP-4 inhibitors have been reported, most of which are derived from α- and β-amino acids that mimic the N-terminal dipeptide residues of natural substrates. Many of the reported DPP-4 inhibitors make a covalent interaction with the Ser630 residue in the S1 pocket.[6] Both sitagliptin and alogliptin (SYR-322)[5e] are notable exceptions. In some DPP-4 inhibitors, the electrophile inherent in a covalent inhibitor in combination with the basic nitrogen necessary for high-affinity binding leads to chemical instability.[7] Therefore, we focused our attention on developing non-covalent inhibitors of DPP-4. In addition, we aimed to design inhibitors that would be potent, selective, and orally active.

We began our design of novel, non-covalent DPP-4 inhibitors with the aid of a co-crystal structure of DPP-4 with compound **1**, commercially available 2-phenylbenzylamine. Although this fragment was found to be a weak inhibitor of DPP-4 (IC_{50} = 30 μM),[8] we considered it to be a very attractive starting point due to its low molecular weight and functional simplicity. In addition, this fragment is related to the 2-phenyl-aminomethyl-heterocycle motif contained within other DPP-4 inhibitors.[9]

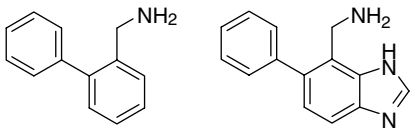

1 **2**

Several important interactions can be observed from the co-crystal structure of compound **1** in the DPP-4 active site (Fig. 1).[10] The basic nitrogen forms a salt bridge between both Glu205 and Glu206, as well as a hydrogen bond with Tyr662; the *ortho*-phenyl ring occupies the S1 pocket formed by Tyr666, Trp659, Tyr631, Val656, Val711, and Tyr662; and a stacking interaction can be observed between the central phenyl ring and Tyr547. The catalytic triad of Ser630, His740, and Asp708 does not interact directly with compound **1**.

Keywords: Dipeptidyl peptidase IV; DPP-4; Benzimidazole; Diabetes; X-ray structure.
* Corresponding author. Tel.: +1 858 731 3598; fax: +1 858 550 0526; e-mail: michael.wallace@takedasd.com

0960-894X/$ - see front matter © 2008 Elsevier Ltd. All rights reserved.
doi:10.1016/j.bmcl.2008.02.071

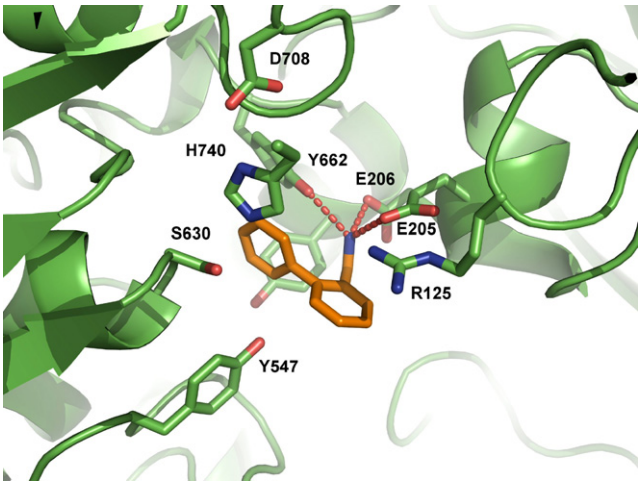

Figure 1. X-ray co-crystal structure of compound **1** bound in the DPP-4 active site.

Utilizing this structure in molecular modeling, we predicted that the bicyclic benzimidazole ring of compound **2** would provide an additional π-stacking interaction with Arg125, while possibly allowing for a hydrogen-bonding interaction with the backbone carbonyl of Glu205. In addition, the benzimidazole ring would provide a drug-like, heterocyclic central scaffold that would be synthetically tractable in further derivatization and SAR development.

The prototype compound **2** showed only a modest improvement in potency (IC_{50} = 12 μM). We reasoned that this compound could adopt a low-energy conformation with an internal hydrogen bond between the benzylic amine and the benzimidazole nitrogen. The molecule would need to overcome such an interaction (at significant energy cost) in order to adopt the proper conformation for optimal binding in the active site of the protein. The N-methylated compound **3a** (Fig. 2) was designed in order to prevent such an internal hydrogen bond, as well as restrict the rotation of the methyl-

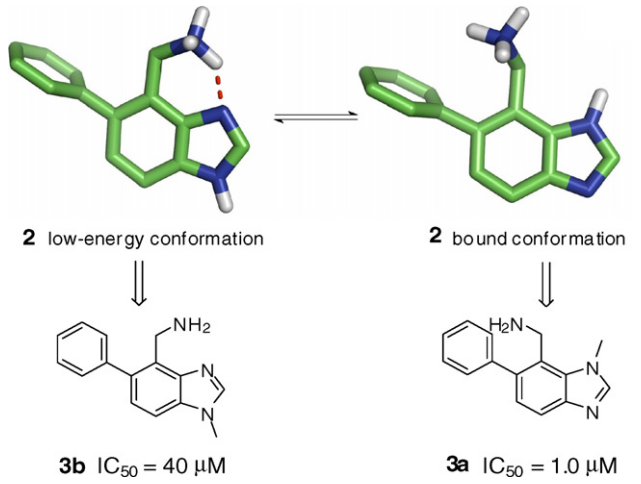

Figure 2. Benzimidazole conformations leading to the design of *N*-methyl benzimidazole isomers **3a** and **3b**.

amine appendage to a range that includes the preferred conformation seen in the crystal structure. Compound **3a** showed a 10-fold increase in potency (IC_{50} = 1.0 μM) over compound **2**, validating our rationale for the design, while the isomer **3b** showed a predicted decrease in potency (IC_{50} = 40 μM). Although the N-alkylated benzimidazole **3a** has lost any possibility of gaining affinity through a hydrogen-bonding interaction with the backbone carbonyl of Glu205, the gain in affinity due to conformational restriction more than compensates for this.

Structural information was used to guide us in our SAR development from compound **3a** (Fig. 3). The position on the phenyl ring that appeared to be most promising for gaining affinity was the *ortho*-position, given the available room to build and possibility for interaction with nearby Arg125. There also appeared to be a small hydrophobic pocket at the *para*-position. Substituents larger than a methyl group at R^1 seemed possible, provided that these larger groups would be able to pack along the backbone of Glu206 and Val207 while directing towards Arg358. Substitution at R^2 seemed promising due to the possibility of creating an interaction with Ser209. Finally, derivatization at R^5 looked highly promising due to the close proximity of Ser630.

The synthesis of the initial core compounds **2** and **3a** is outlined in Scheme 1.[11] 2-Amino-6-chloro-3-nitro-benzonitrile **4a** (R^1 = H) was prepared according to the method of Goldberg and coworkers.[12] A Suzuki reaction with phenylboronic acid gave compound **5a** (R = H), and subsequent nitro reduction by hydrogenation led to intermediate **6a**. Acid catalyzed condensation with formic acid gave compound **7a** (R^2 = H), which was reduced by high-pressure hydrogenation to produce compound **2**. Alkylation of intermediate **7a** with dimethylsulfate followed by hydrogenation yielded compounds **3a** and **3b** as a 2:1 ratio of isomers.

The original synthetic scheme was expanded and modified to allow for SAR development at multiple positions on the core. The general route outlined in Scheme 1 was used in the syntheses of compounds **8**–**24**. The R^1 groups were installed from the start of the sequence by the selective S_NAr displacement of the C-2 chlorine of 2,6-dichloro-3-nitro-benzonitrile with primary amines. Subsequent Suzuki reactions with R-substituted arylboronic acids led to intermediates **5**. Nitro reductions were carried out with hydrogenation as before, or by using

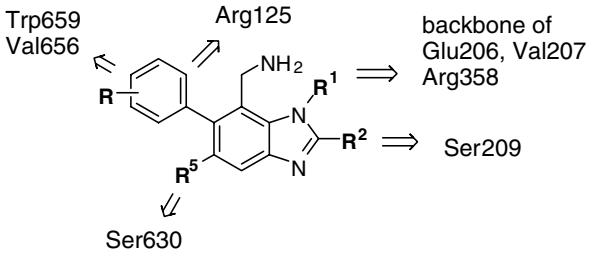

Figure 3. SAR strategy for benzimidazole DPP-4 inhibitors.

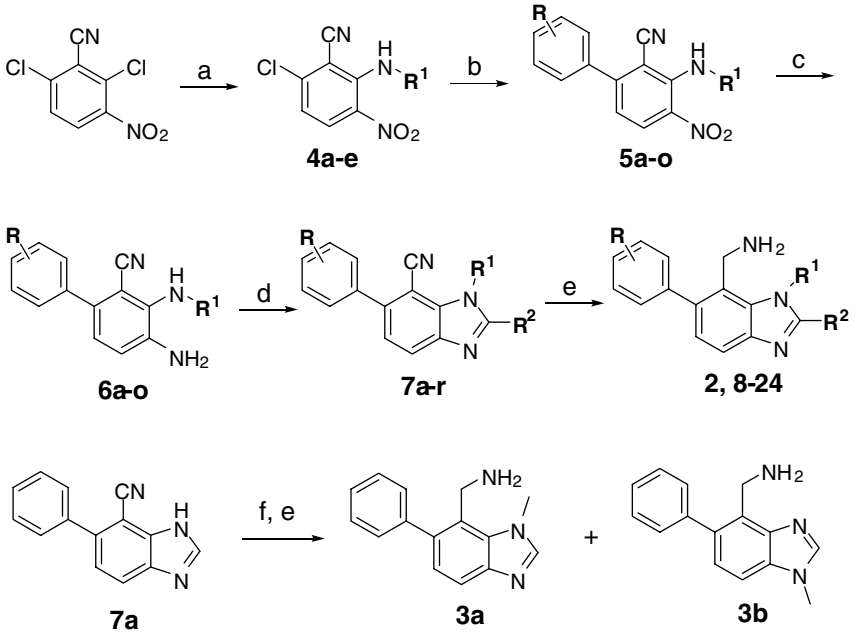

Scheme 1. Synthesis of compounds **2–24**. Reagents and conditions: (a) R^1NH_2, THF; (b) R-Ph-$B(OH)_2$, Pd_2dba_3, DavePhos, K_3PO_4, DMA, 68 °C; (c) H_2, Pd/C, MeOH; or Fe, HOAc; (d) R^2CO_2H, PPA; (e) H_2, Pd/C, HOAc, MeOH, 50 p.s.i.; or 1—BH_3·THF, reflux, 1 h; 2—HCl; (f) dimethylsulfate, K_2CO_3.

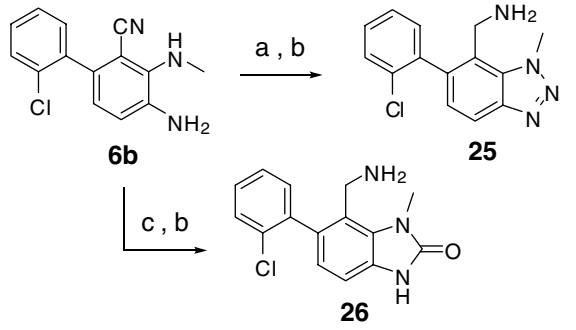

Scheme 2. Synthesis of benzotriazole and benzimidazolone compounds **25** and **26**. Reagents and conditions: (a) $NaNO_2$, HCl; (b) 1—BH_3·THF, reflux, 1 h; 2—HCl; (c) CDI, THF.

iron in acetic acid in instances with halogen-containing substrates. The resulting diamine compounds **6** were heated with carboxylic acids (or esters) in the presence of a catalytic amount of PPA to give the benzimidazoles **7** with R^2 groups in place. Finally, nitrile reductions occurred optimally through either high-pressure hydrogenation or borane reduction to yield the final compounds **8–24**.

The synthetic scheme was amenable to simple core modifications as well (Scheme 2). The benzotriazole **25** and benzimidazolone **26** were synthesized by treatment of the aniline **6b** (R = 2-Cl, R^1 = Me) with sodium nitrite or carbonyldiimidazole, respectively, followed by borane reduction of the nitrile to give the desired amines.

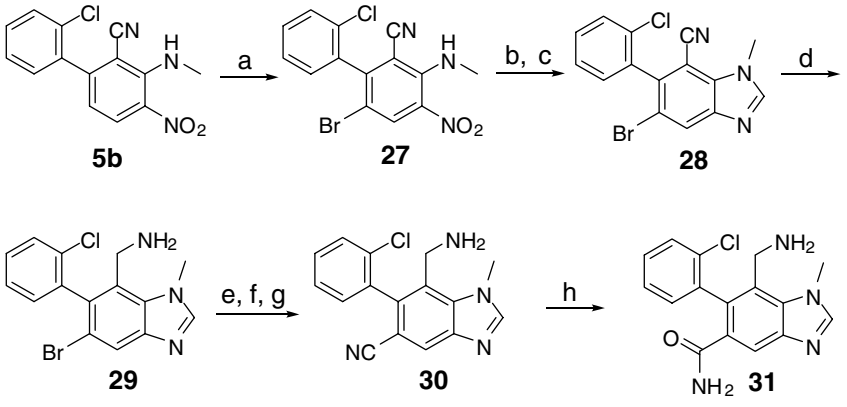

Scheme 3. Synthesis of compounds **29–31**. Reagents and conditions: (a) Br_2, HOAc, 88 °C; (b) Fe, HOAc; (c) formic acid, PPA; (d) 1—BH_3·THF, reflux; 2—HCl; (e) BOC_2O; (f) $Zn(CN)_2$, Pd_2dba_3, DavePhos, K_3PO_4, DMA, 92 °C; (g) TFA, CH_2Cl_2; (h) H_2O_2, KOH, MeOH.

Table 1. Selected data for benzimidazole analogues: R and R^1-modified compounds

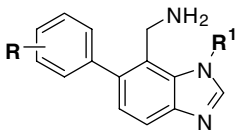

Compound	R	R^1	DPP-4 IC_{50} (μM)	DPP-8 IC_{50} (μM)	RLM/HLM $t_{1/2}$ (min)
3a	H	Me	1.0	63	46/93
8	2-CH_2OH	Me	0.4	NT	39/100
9	2-Cl	Me	0.063	50	57/>200
10	2-$CONH_2$	Me	4.0	NT	NT/NT
11	2-OMe	Me	2.0	NT	NT/NT
12	2-OH	Me	1.6	NT	NT/NT
13	2-Me	Me	0.098	80	28/183
14	2,4-Di-Cl	Me	0.062	25	46/>200
15	2-Cl, 5-F	Me	0.32	NT	NT/NT
16	2,4-Di-F	Me	0.79	NT	NT/NT
17	2,4-Di-Cl	H	0.63	32	46/129
18	2,4-Di-Cl	Et	0.066	50	42/>200
19	2-Cl	CH_2CH_2OH	0.096	20	32/>200
20	2-Cl	Bn	0.102	>100	4/8

NT, not tested.

Table 2. Selected data for benzimidazole analogues: R^2 and R^5-modified compounds

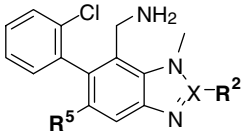

Compound	X	R^2	R^5	DPP-4 IC_{50} (μM)	DPP-8 IC_{50} (μM)	RLM/HLM $t_{1/2}$ (min)
9	C	H	H	0.063	50	57/>200
21	C	Me	H	0.160	NT	7/>200
22	C	Et	H	0.097	32	2/>200
23	C	CH_2OCH_3	H	0.066	40	11/>200
24	C	3-Pyridyl	H	0.011	4.0	26/96
25	N		H	0.061	40	13/29
26	C=O		H	0.052	>100	76/>200
29	C	H	Br	0.050	>100	24/176
30	C	H	CN	0.008	>100	38/>200
31	C	H	$CONH_2$	0.032	32	>200/>200

NT, not tested.

The synthesis of R^5-substituted compounds **29**–**31** is illustrated in Scheme 3. Bromination of intermediate **5b** selectively produced compound **27**. Nitro reduction, benzimidazole formation, and nitrile reduction were carried out as previously described to produce compound **29**. Boc-protection of the resulting amine was necessary prior to palladium-catalyzed cyanation of the aryl bromide, and subsequent Boc-deprotection gave compound **30**. Finally, hydrolysis of the nitrile with basic peroxide yielded the benzamide compound **31**. Compounds **29**–**31** were determined to exist as diastereomeric mixtures of atropisomers by chiral SFC analysis.[13] Experimental data were collected for the compound mixtures.

Results of initial SAR development for the series are shown in Table 1. Substitution at the *ortho*-position of the phenyl ring with a methyl or preferably chloro group (compounds **13** and **9**, respectively) provided a substan-

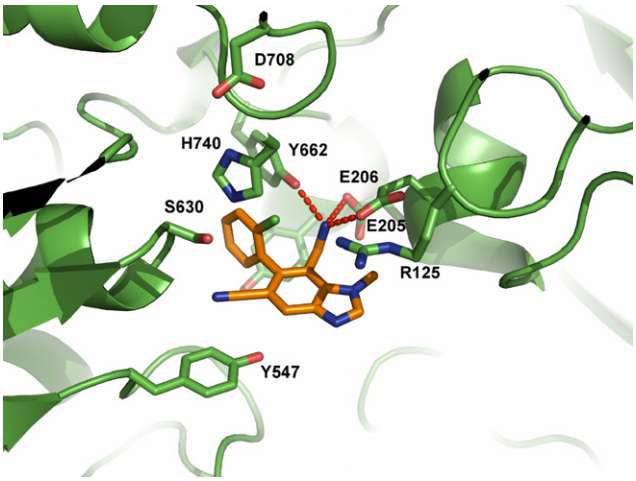

Figure 4. X-ray co-crystal structure of compound **30** in the DPP-4 active site.

Table 3. Selected PK parameters for compounds **14**, **26**, and **30**

Compound	Dose iv/oral (mg/kg)	iv $t_{1/2}$ (h)	Oral $t_{1/2}$ (h)	AUC_{po} (μg h/mL)	V_{dss} (mL/kg)	F (%)
14	0.8/8	7.0	4.4	11.5	4808	100
26	0.7/8.4	4.2	4.0	9.0	1137	49
30	1.0/11.6	3.8	2.9	22.1	1073	122

tial (>10×) boost in potency. Larger or more polar groups were not as well tolerated. The addition of a chlorine at the *para*-position had little effect. SAR at the R^1 position demonstrated that groups larger than methyl could be tolerated, but no additional improvement in activity was observed.

Once the R and R^1 groups were optimized (R = 2-Cl, R^1 = Me), we turned our attention to SAR work at R^2 and R^5 (Table 2). Substitution at R^2 with a 3-pyridyl group (compound **24**) resulted in a sixfold increase in potency (IC_{50} = 11 nM), demonstrating the utility in optimal engagement of Ser209. In addition, the central core could be modified to the benzotriazole **25** or the benzimidazolone **26** without significant change in activity. Substitution at R^5 proved to be highly productive, with the 5-cyano group (compound **30**) imparting the greatest improvement in enzyme inhibition (IC_{50} = 8 nM). This low molecular weight compound also displayed excellent selectivity over the related S9B protease DPP-8.

The co-crystal structure of compound **30** in the DPP-4 active site is shown in Figure 4.[14] A single atropisomer of the compound preferentially co-crystallizes with the enzyme. In addition to the interactions described for compound **1**, the benzimidazole ring displays a π-stacking interaction with Arg125. The chlorine on the phenyl ring favorably increases the dihedral angle of the bicyclic system and also makes an electrostatic interaction with Arg125. The 5-cyano group favorably interacts with neighboring residues and locks the orthogonal conformation of the bicyclic system.

After acceptable enzymatic activity and microsomal stability were demonstrated for compounds **14**, **26**, and **30**, the pharmacokinetic properties of these compounds were determined in rats (Table 3). Compound **14** showed long half-life, low clearance, and excellent oral bioavailability. Compounds **26** and **30** showed moderate half-lives, low clearance, and moderately high volume of distribution. The oral bioavailability was determined to be 49% for compound **26** and in excess of theoretical 100% for compound **30**.

In summary, we have utilized structure-based design to build a novel series of non-covalent benzimidazole-based DPP-4 inhibitors from a small fragment lead. SAR development led to the discovery of multiple compounds which are potent and selective while maintaining excellent physical properties and drug-like characteristics. We have developed highly versatile synthetic schemes for the rapid development of SAR around this core.

Acknowledgments

The authors appreciate the drug-discovery expertise of Jeffrey Stafford and Stephen Kaldor. We thank G. Sridhar Prasad, Gyorgy Snell, Melinda Manuel, Lu Zeng, and Derek B. Laskar for their valuable experimental assistance. We also thank Andrew Jennings for technical assistance in computational chemistry. The X-ray crystallography data reported here are based on research conducted at the Advanced Light Source (ALS). ALS is supported by the Director, Office of Science, Office of Basic Energy Sciences, Materials Sciences Division, of the U.S. Department of Energy (DOE) under Contract No. DE-AC03-76SF00098 at Lawrence Berkeley National Laboratory. We thank the staff at ALS for their excellent support in the use of the synchrotron beam lines.

References and notes

1. (a) Yaron, A.; Naider, F. *Crit. Rev. Biochem. Mol. Biol.* **1993**, *28*, 31; (b) Heins, J.; Welker, P.; Schönlein, C.; Born, I.; Hartrodt, B.; Neubert, K.; Tsuru, D.; Barth, A. *Biochim. Biophys. Acta* **1988**, *954*, 161.
2. Drucker, D. J. *Expert Opin. Investig. Drugs* **2003**, *12*, 87.
3. (a) Gwaltney, S. L.; Stafford, J. A. *Ann. Rep. Med. Chem.* **2005**, *40*, 149; (b) Green, B. D.; Flatt, P. R.; Bailey, C. J. *Diabetes Vasc. Dis. Res.* **2006**, *3*, 159; (c) Drucker, D. J.; Nauck, M. A. *Lancet* **2006**, *368*, 1696; (d) Ahrén, B. *Diabetes Care* **2007**, *30*, 1344.
4. (a) Herman, G. A.; Bergman, A.; Liu, F.; Stevens, C.; Wang, A. Q.; Zeng, W.; Chen, L.; Snyder, K.; Hilliard, D.; Tanen, M.; Tanaka, W.; Meehan, A. G.; Lasseter, K.; Dilzer, S.; Blum, R.; Wagner, J. A. *J. Clin. Pharmacol.* **2006**, *46*, 876; (b) Kim, D.; Wang, L.; Beconi, M.; Eiermann, G. J.; Fisher, M. H.; He, H.; Hickey, G. J.; Kowalchick, J. E.; Leiting, B.; Lyons, K.; Marsilio, F.; McCann, M. E.; Patel, R. A.; Petrov, A.; Scapin, G.; Patel, S. B.; Roy, R. S.; Wu, J. K.; Wyvratt, M. J.; Zhang, B. B.; Zhu, L.; Thornberry, N. A.; Weber, A. E. *J. Med. Chem.* **2005**, *48*, 141.
5. (a) Ahrén, B.; Gomis, R.; Standl, E.; Mills, D.; Schweizer, A. *Diabetes Care* **2004**, *27*, 2874; (b) Ahrén, B. *Expert Opin. Investig. Drugs* **2006**, *15*, 431; (c) Villhauer, E. B.; Brinkman, J. A.; Naderi, G. B.; Burkey, B. F.; Dunning, B. E.; Prasad, K.; Mangold, B. L.; Russell, M. E.; Hughes, T. E. *J. Med. Chem.* **2003**, *46*, 2774; (d) Augeri, D. J.; Robl, J. A.; Betebenner, D. A.; Magnin, D. R.; Khanna, A.; Robertson, J. G.; Wang, A.; Simpkins, L. M.; Taunk, P.; Huang, Q.; Han, S.-P.; Abboa-Offei, B.; Cap, M.; Xin, L.; Tao, L.; Tozzo, E.; Welzel, G. E.; Egan, D. M.; Marcinkeviciene, J.; Chang, S. Y.; Biller, S. A.; Kirby, M. S.; Parker, R. A.; Hamann, L. G. *J. Med. Chem.* **2005**, *48*, 5025; (e) Feng, J.; Zhang, Z.; Wallace, M. B.; Stafford, J. A.; Kaldor, S. W.; Kassel, D. B.; Navre, M.; Shi, L.; Skene, R. J.; Asakawa, T.; Takeuchi, K.; Xu, R.; Webb, D. R.; Gwaltney, S. L. *J. Med. Chem.* **2007**, *50*, 2297.

6. (a) Engel, M.; Hoffmann, T.; Wagner, L.; Wermann, M.; Heiser, U.; Kiefersauer, R.; Huber, R.; Bode, W.; Demuth, H.-U.; Brandstetter, H. *Proc. Natl. Acad. Sci. U.S.A.* **2003**, *100*, 5063; (b) Oefner, C.; D'Arcy, A.; MacSweeney, A.; Pierau, S.; Gardiner, R.; Dale, G. E. *Acta Crystallogr.* **2003**, *D59*, 1206.
7. Magnin, D. R.; Robl, J. A.; Sulsky, R. B.; Augeri, D. J.; Huang, Y.; Simpkins, L. M.; Taunk, P. C.; Betebenner, D. A.; Robertson, J. G.; Abboa-Offei, B. E.; Wang, A.; Cap, M.; Xin, L.; Tao, L.; Sitkoff, D. F.; Malley, M. F.; Gougoutas, J. Z.; Khanna, A.; Huang, Q.; Han, S.-P.; Parker, R. A.; Hamann, L. G. *J. Med. Chem.* **2004**, *47*, 2587.
8. DPP-4 Assay: Solutions of test compounds in varying concentrations ($\leqslant$10 mM final concentration) were prepared in DMSO and then diluted into assay buffer comprising: 20 mM Tris, pH 7.4; 20 mM KCl; and 0.1 mg/mL BSA. Human DPP-4 (0.1 nM final concentration) was added to the dilutions and pre-incubated for 10 min at ambient temperature before the reaction was initiated with A-P-7-amido-4-trifluoromethylcoumarin (AP-AFC; 10 μM final concentration). The total volume of the reaction mixture was 10–100 μL depending on assay formats used (384 or 96 well plates). The reaction was followed kinetically (excitation $\lambda = 400$ nm; emission $\lambda = 505$ nm) for 5–10 min or an end-point was measured after 10 min. Inhibition constants (IC_{50}) were calculated from the enzyme progress curves using standard mathematical models.
9. (a) Peters, J.-U.; Weber, S.; Kritter, S.; Weiss, P.; Wallier, A.; Boehringer, M.; Hennig, M.; Kuhn, B.; Loeffler, B.-M. *Bioorg. Med. Chem. Lett.* **2004**, *14*, 1491; (b) Peters, J.-U.; Hunziker, D.; Fischer, H.; Kansy, M.; Weber, S.; Kritter, S.; Müller, A.; Wallier, A.; Ricklin, F.; Boehringer, M.; Poli, S. M.; Csato, M.; Loeffler, B.-M. *Bioorg. Med. Chem. Lett.* **2004**, *14*, 3575; (c) Rummey, C.; Nordhoff, S.; Thiemann, M.; Metz, G. *Bioorg. Med. Chem. Lett.* **2006**, *16*, 1405.
10. Protein Data Bank code is 3CCB.
11. Full experimental procedures for all syntheses are contained within the following patent application: Feng, J.; Gwaltney, S. L.; Wallace, M. B.; Zhang, Z. PCT Int. Patent Appl. WO 05/118555, **2005**.
12. Goldberg, D. R.; Butz, T.; Cardozo, M. G.; Eckner, R. J.; Hammach, A.; Huang, J.; Jakes, S.; Kapadia, S.; Kashem, M.; Lukas, S.; Morwick, T. M.; Panzenbeck, M.; Patel, U.; Pav, S.; Peet, G. W.; Peterson, J. D.; Prokopowicz, A. S.; Snow, R. J.; Sellati, R.; Takahashi, H.; Tan, J.; Tschantz, M. A.; Wang, X.-J.; Wang, Y.; Wolak, J.; Xiong, P.; Moss, N. *J. Med. Chem.* **2003**, *46*, 1337.
13. Zeng, L.; Xu, R.; Laskar, D. B.; Kassel, D. B. *J. Chromatogr. A* **2007**, *1169*, 193.
14. Protein Data Bank code is 3CCC.